C25

A Cooling System for Enhanced Solar Module Efficiency

Alretaj AlBarjas **Fatmah AlAnsari** *Student Member ASHRAE* **Joury AlKhateeb**

Renad AlZamel **Abdulazim Falah, PhD** **Nawaf AlJuwayhel, PhD**

ABSTRACT

As the temperature rises above 25°C, the efficiency of a crystalline photovoltaic module decreases by around 0.5% per 1°C increase. The purpose of this study is to develop a passive cooling system for a crystalline photovoltaic module to reclaim its lost efficiency at high temperatures, whilst not negatively affecting it during diurnal or seasonal temperature variations. The study was done numerically using COMSOL Multiphysics® software of the proposed passive cooling system. The cooling method chosen is a hybrid arrangement of two layers of phase change material with two different melting temperatures and fins. The parameters of concern are the melting temperature of the PCM chosen, the amount of PCM, the profile and distribution of the fins, the thermal conductivity of the fins and PCM, and the efficiency of the overall cooling system. The results of the numerical analysis proved the cooling method to be successful in lowering the temperature of the panel, year-round.

INTRODUCTION

In the 21st century, humans lead luxurious lives enabled by the exploitation of the natural resources of the planet. Electricity revolutionized the way humans live their day-to-day lives. In recent years, oil and natural gas have been the leading form of energy source worldwide. However, the extraction and burning of such fuels has taken its toll on the environment. Solar energy has immense potential in Kuwait, as the country is exposed to extremely high solar irradiance, yearly. Solar panels are made of smaller units called solar cells. Soler cells are commonly made from silicon, which is a semiconducting material (Howell 2023). A layer of the semiconducting material is doped with small quantities of boron, which has three valance electrons making the overall charge of the semiconducting material positive. A negative charge is made by doping the silicon with phosphorous, which has an excess of free electrons. The negative and positive semiconducting material make up what is termed a pn-junction. When the photons coming from sunlight reach the solar cell, the electrons in the semiconducting material which were in a low energy state are excited, and in turn move, generating an electrical current as a result, this process is known as the Photovoltaic Effect, hence the name Photovoltaic cell (PV) was given to the solar cells. The difference between the low energy state and the excited state is what could determine the power produced by the PV cell. The higher the difference, the higher power output. At a high temperature, the electron is already in a slightly excited state due to thermal energy gain, as a result, the electron behaves differently because of the decrease in the difference between these two levels, thus the efficiency decreases (Boyle 2004). A temperature coefficient measures the power output drop when the module's temperature is above 25°C or the standard test condition (Perez 2022), and it is usually -0.5% for every 1°C increase. Implementing effective cooling mechanisms plays a crucial role in enhancing the energy efficiency of PV solar modules by reducing the operating temperature of their surfaces and ensuring optimal operation. Consequently, solar panels demonstrate superior performance in colder climates compared to hotter environments. Numerous researchers have explored cooling methods to address the temperature concerns associated with PV solar panels. Active, passive, and forced cooling methods were discussed by researchers such as natural or forced air cooling, active water cooling, and so on. Active cooling methods hinder the power production of the cells

Alretaj AlBarjas, Fatmah AlAnsari, Joury AlKhateeb, Renad AlZamel, Abdulazim Falah, and Nawaf AlJuwayhel are affiliated with Kuwait University, Kuwait City, Kuwait.

as some of the power is fed for pumping or to power the fan in the case of forced ventilation. Passive cooling systems, on the other hand, fall behind in reducing the temperature.

Odehand and Behnia cooled a PV panel with water with a water trinkling systems and the electrical output was increased by 4-10%. Active water spraying can reduce the PV cell temperature and has relatively higher heat transfer rates, but the power consumption, the installation, and maintenance costs are high. Similarly, forced ventilation consumes power to operate and has high maintenance and installation costs, however unlike natural ventilation, forced ventilation allows for more temperature reduction, as was found by Yun et al. where a temperature between 20-30°C was achieved.

Passive cooling includes liquid immersion where solar cells are immersed in a dielectric liquid which maintains their temperature between 30-45°C, as was found by Zhu et al. Fins or heat sinks are another method of passive cooling where the buoyancy forces allow the panel to exchange heat with ambient air through convection. Fins require no maintenance, and the installation costs are minimum. Also, heat sinks reduced the temperature of a panel by an average of 7.5°C as was found by Krstic et al. Another passive cooling method is the addition of phase change material (PCM). Usually PCM are installed in a 4 [cm] enclosure on the back of the PV module (Tao, et al. 2019). PCMs are materials that act as a latent storage material. In other words, PCM store heat as they melt and release that heat as they solidify at temperatures below their melting point. The PCM layer thickness and its melting temperature are vital properties in determining the amount of heat dissipated, and those properties are expected to differ in different climatic conditions. Usually, a single layer of PCM is incorporated, however Chandel and Agarwal suggested the study of PCM with two different melting points, one to regulate the temperature of the module at diurnal temperature variations and another to adjust the temperature at peak temperatures.

This research study aimed to assess the impact of incorporating a phase change material and fins into a PV module. The chosen cooling approach involved a hybrid configuration consisting of two layers of PCM with distinct melting temperatures, along with the implementation of fins. The investigation focused on key parameters, including the PCM's melting temperature, PCM quantity, fin profile and distribution, thermal conductivity of both the fins and PCM, and the overall cooling system efficiency. The outcomes derived from numerical analysis substantiated the effectiveness of the cooling method in consistently reducing the panel's temperature throughout the year.

THE PHOTOVOLTAIC EFFICIENCY MODEL

It is known that as the panel's temperature rises above 25°C, the efficiency of the panels decreases by 0.5% per 1°C increase (Chandel & Agarwal 2017). The instantaneous temperature dependent electrical efficiency of the PV module can be expressed as

$$\eta_p = \eta_{Tref}[1 - \beta_{ref}(T_p - T_{ref})] \tag{1}$$

where η_{ref} is the module efficiency at the reference temperature of 25°C, β_{ref} is the temperature coefficient which has a value of 0.004 K^{-1} for crystalline silicon modules, and T_p is the panel temperature (Dubey, et al. 2013).
The output power can be calculated in terms of the efficiency as follows

$$P = \eta_p A_p I \tag{2}$$

where A_p is the area of the panel and I is the solar irradiance reaching the panel.

NUMERICAL SIMULATION

COMSOL Multiphysics® software was used for the design analysis of 3D models. The simulated module was based on a RECOM® 360-W monocrystalline panel with a module efficiency of 18.55%. A numerical analysis was also done using COMSOL to determine the optimum hybrid system configuration, which will be first tested on the 21st of June before the yearly comparison. The physics involved in the simulation are heat transfer in solids and fluids with phase change material and surface-to-surface radiation using solar position and local coordinates. The coordinates chosen correspond to a house in AlNuzha, Kuwait. Figure 1 shows the dimensions of each of the layers used to simulate the PV module and table 1 lists the properties used.

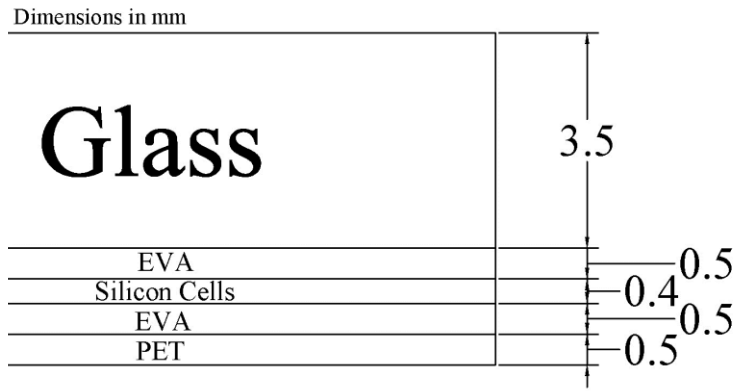

Figure 1 Layers of the simulated PV module.

Table 1. The thermal properties of the materials of the simulated PV module

Material	Density [kg/m³]	Thermal Conductivity [W/(m·K)]	Heat Capacity [J/(kg·K)]
Glass (Connor, 2021)	2500	1	840
EVA (J & T 2018 and Brydson 1999)	35	0.04	1400
Silicon (single-crystal, isotropic) (COMSOL 2023)	2329	130	700
PET (Connor 2021)	1350	0.3	1250

BOUNDARY CONDITIONS

1. The surfaces of the panel are subjected to external natural convection for inclined plates with the ambient temperature of air.
2. The surfaces of the panel are subjected to external radiation with the ambient temperature.
3. The ambient properties were adapted from ASHRAE 2017 Meteorological Data, where the hourly temperatures are known.
4. The hourly solar irradiance is known for the 21st day of each month and was calculated with the solar angles using MATLAB.

ASSUMPTIONS

1. There is no heat being generated by the PV module.
2. The air velocity is the same on all sides of the PV module and the turbulent effects are not considered.
3. The glass of the PV module is not opaque to any spectral wavelength.
4. On the surface of the fins, forced and natural convention heat transfers prevail over the radiation and thus the radiation was neglected.

5. The ground chosen is built in COMSOL material library as Soil.
6. The initial temperature is 27°C.

RESULTS AND DISCUSSION
OPTIMUM HEATSINK DESIGN

Fin profile. A comparison was made between three different typical fin profiles which are conventional fins of a rectangular cross-section, trapezoidal fins, and cylindrical fins. The three fin solutions were compared against each other on June 21st and at 2:00 PM; all parameters except the profile of the fin was constant, including the fin length. Table 2 lists the results of the three studies. The thicknesses of the trapezoidal and rectangular fins were 0.5 [mm] with the same number of fins, and the diameter of the cylindrical fins was 50 [mm]. Also, all fins had the length of 100 [mm].

Table 2. Comparison between the different fin profiles

	Rectangular Fins	Cylindrical Fins	Trapezoidal Fins
$T_{avg,\,PET}$ [°C]	49.66	50.28	48.72
Total fins mass [kg]	7.48	32.32	7.93

From table 2 and upon comparing the three results it is obvious that the rectangular and trapezoidal profiles performed better than the cylindrical fins, thus the latter was eliminated. The choice was between rectangular and trapezoidal fins. There is a difference of 0.94°C and a mass difference between the two profiles. Since the two profiles had similar performances, the rectangular fins were chosen as they are easier to manipulate and to manufacture, considering that both profiles use almost the same amount of aluminum, with the trapezoidal almost 500 [g] more material.

Fin Length and Thickness At 2:00 PM on June 21st, the average back surface temperature of the reference PV module was 53.046°C. figure 2a represents the average temperature of the back panel as the fin length is increased from 50-350 [mm] with an increment of 50 [mm] and the number of fins, spacing, and thickness were kept constant. When restricting radiation from interacting with the fins, it was found that the longer the fin the more heat is dissipated and the lower is the temperature. It is also worth noting that all fin lengths successfully reduced the temperature from the reference PV temperature of 53.046°C. Figure 2b shows the relation between the average back surface temperature and the thickness of fins. Figure 3 shows the final optimum fin setup.

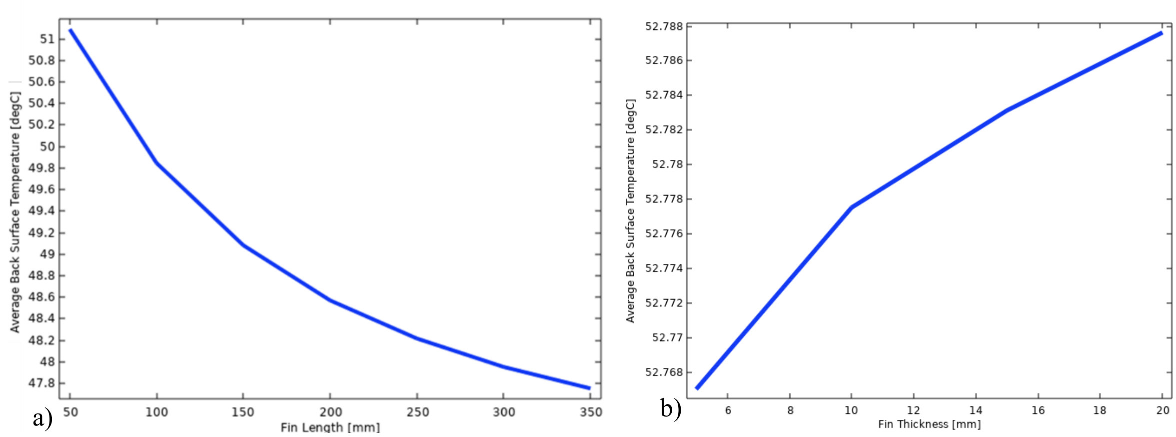

Figure 2 (a) The average temperature of the back surface against an increasing fin length and (b) The average temperature of the back surface against an increasing fin thickness.

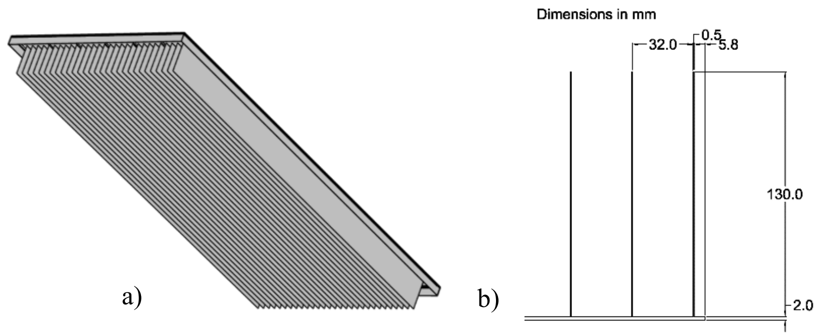

Figure 3 (a) A 3D model of the optimum fin design and (b) 2D drawing of the optimum fin design.

Number of Fins and Distribution. Next, to decide on the distribution and number of fins. It was decided to cover the entire width of the panel with longitudinal rectangular fins of a thickness of 0.5 [mm]. At the same time, the heat sink must not be compact enough to have considerable radiative heat exchange. Thus, a spacing of 32 [mm] and 29 fins covered the panel acceptably. Figure 4b shows the 2D drawing of the designed fins arrangement. Where the final fin length was 130 [mm].

OPTIMUM PCM ARRANGEMNET

Table 3. Measured wax densities

	Density [kg/m^3]	
Wax	**Solid state**	**Liquid state**
Natural Soy wax	733.33	957.15
Paraffin Wax	800	833.33

Table 3 lists the measured densities of the waxes to be used as the PCM in the cooling system. Figure 5a shows the simulated behavior of an uncooled panel on the 21st day of each month. A parametric study was done to find the optimum two-layer PCM configuration, if any. The melting temperature of the two layers were varied independently of each other as well as their thicknesses. All PCM arrangements resulted in at least a reduction of 4.3°C, which is quite significant, considering it was calculated during the summer solstice. Also, between the different 64 results of the parametric study none of the resulting average temperature exceeded 48.79°C. and the difference between the temperatures was in the decimal fractions only. Consequently, it was decided to use PCM with two different melting temperatures both of which have a layer thickness of 10 [mm]. The reason for choosing layers with two different melting temperatures is that as is evident from figure 4a, the back surface temperature in winter and parts of autumn and spring does not reach 52°C, which is the melting temperature of paraffin wax, which justifies the addition of the 43°C melting temperature soy wax. Likewise, in summer the temperature is much higher than 43°C at peak temperature hours, which demands the addition of paraffin with its 52°C melting temperature to be able to store that heat during those elevated temperatures. Figure 4b shows the final set up of the hybrid system with the two 10 [mm] layer PCM.

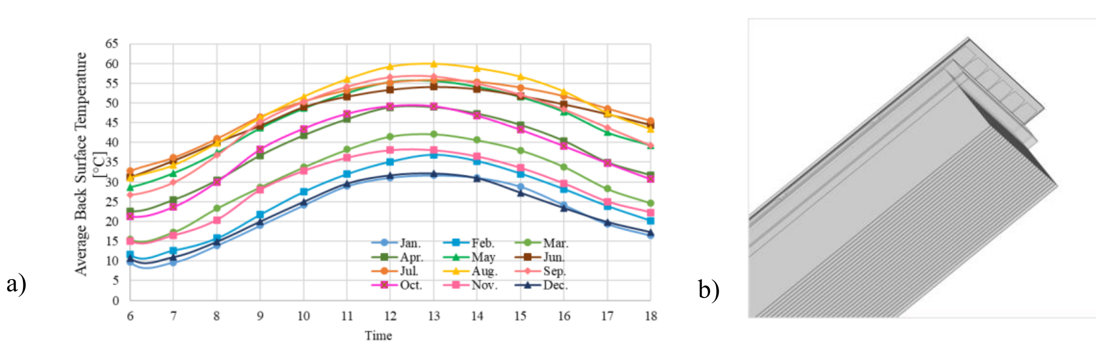

Figure 4 (a) The average temperature on the 21st day of each month and (b) the final hybrid geometry.

PERFORMANCE OF THE COOLING SYSTEM

The hybrid cooled panel was simulated on the 21st of each month of the year from 6:00 AM to 6:00 PM. The results of the average temperature of the back surface of the panel starting from March until August with the corresponding efficiency is shown in figure 5.

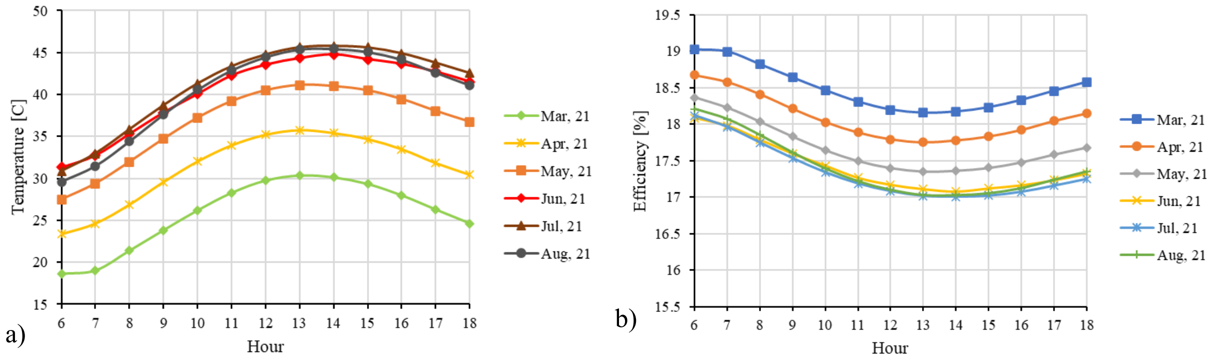

Figure 5 Numerical Results from March to August of (a) The average temperature and (b) The efficiency

The hybrid cooled panel has the same behaviour as the uncooled panel, but the temperature range has dropped. In the spring and summer at noon, the highest temperature range for the uncooled was between 40 and 60°C. Whereas for the hybrid cooled panel, the highest temperature range at noon is now between 30 and 45°C. As for the efficiency, even during the hottest months, the hybrid cooled panel's efficiency did not decrease below 17%. A comparison was made between the efficiencies at 1 PM of the uncooled and hybrid cooled panels during the hottest months of the year in Kuwait, of which the results of the efficiencies are shown in table 4.

Table 4. The Efficiency Analysis During the Hottest Months in Kuwait

[%]	May	June	July	August	September
Module Efficiency	18.55	18.55	18.55	18.55	18.55
Minimum Uncooled Efficiency	16.276	16.390	16.264	15.956	16.196
Efficiency Drop	2.274	2.160	2.286	2.594	2.354
Minimum Hybrid Efficiency	17.354	17.115	17.018	17.036	17.271
Efficiency Rise	1.078	0.724	0.754	1.080	1.075
Percentage of Reclaimed Efficiency	47.42	33.54	32.97	41.64	45.67

It is evident that the highest percentage recovered of the dropped efficiency was obtained in May, where the hybrid cooled panel had an efficiency 1.08% higher than the uncooled, making the panel gain back 47.4% of the dropped efficiency. Coming after May, the efficiency gain in a descending order was in September, August, June, and then July. The results of the average temperature of the back surface of the panel starting from September until February are shown in figure 6.

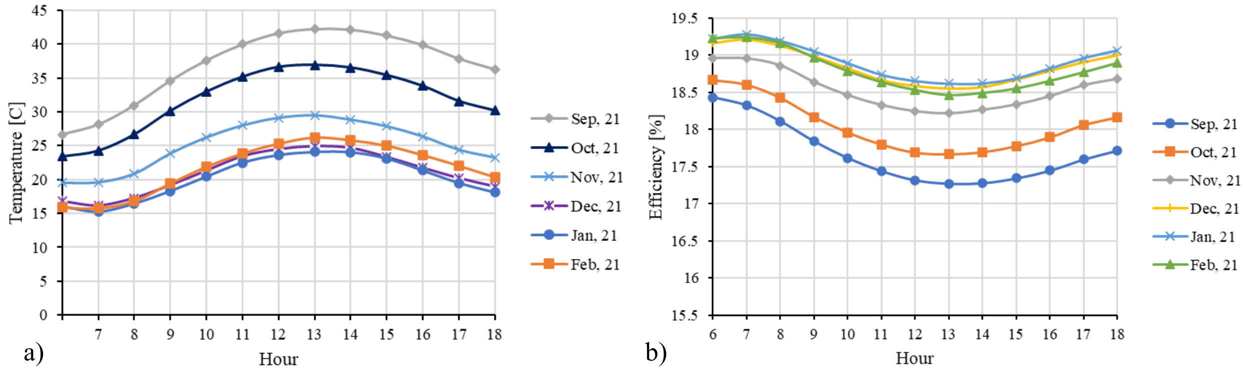

Figure 6 Numerical Results from September to February of (a) The average temperature and (b) The Efficiency.

For the uncooled panel in September and October, the panel's temperature at noon reached 56 and 49°C, respectively. From November to February, the average temperature ranged between 30 and 40°C. For the hybrid cooled system, it is noticed that at noon of September and October, temperature reaches 42 and 36°C, respectively. Whereas from November until February at noon, the range drops to 24 to 30 °C. As for the efficiency, it increased above the manufacturer's efficiency in December, January, and February during all sun hours. For September, October, and November, the efficiency at noon ranges between 17.3% and 18.3%. This performance of the hybrid cooling system satisfies the design constraint of not negatively affecting the panels behaviour during regular conditions. To better understand the effect of the efficiency rise, the electrical energy production during the 21st of each month was calculated for an uncooled panel and a hybrid cooled panel as demonstrated in table 5.

Table 5. The Energy Production During the 21st of each Month

	Energy [Watt. Hour]			
Day	**Uncooled**	**Hybrid Cooled**	**Difference**	**Increase in Energy Production [%]**
Jan, 21	2331.20	2379.00	47.80	2.05
Feb, 21	2588.40	2661.00	72.60	2.80
Mar, 21	2627.60	2720.00	92.40	3.52
Apr, 21	2487.20	2593.00	105.80	4.25
May, 21	2332.30	2448.00	115.70	4.96
Jun, 21	2278.90	2359.00	80.10	3.51
Jul, 21	2279.50	2366.00	86.50	3.79
Aug, 21	2310.70	2429.00	118.30	5.12
Sep, 21	2375.50	2501.00	125.50	5.28
Oct, 21	2361.20	2459.00	97.80	4.14
Nov, 21	2280.70	2341.00	60.30	2.64
Dec, 21	2216.00	2257.00	41.00	1.85

It is evident that for each month, the daily energy generated of the hybrid cooled panel is higher than the uncooled panel. This is attributed to the efficiency rise. The maximum amount of energy gain is obtained on September 21st which is equal to 125.5 [Watt. Hour] representing a 5.28% regain in the daily energy production. Next, August, May, April, October have gain percentages that are higher than 4%. In March, June, and July, the energy gain percentages are 3.52%, 3.51%, and 3.79% respectively. The energy gain from November until February is less than the other months which is expected since the uncooled panel has a good performance in winter and the temperature rise is not significant, but the hybrid cooled panel outperformed the uncooled panel.

VALIDATION OF THE MODEL

The numerical model was validated on the 15th of May with an experimental model with the same setup. Figure 7 shows the experimental model and the comparison with the numerical model for the hours 2-5 PM.

a)

b)

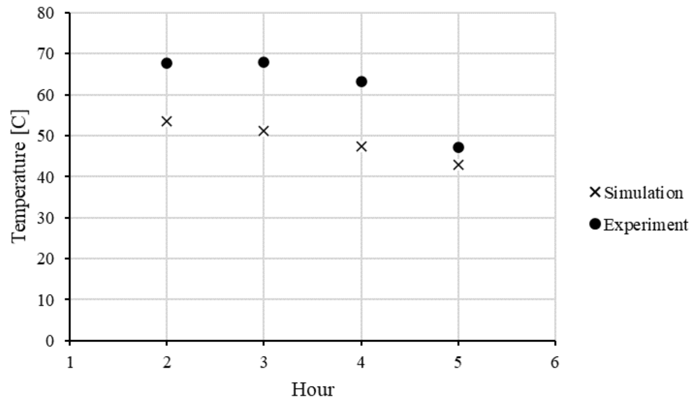

Figure 7 (a) Experimental panel at its test location and (b) comparison between the numerical and experimental results on May 15 of the uncooled panel.

The general trend between the experimental data and model production closely matches, but there's an approximate 25% difference in absolute values. This discrepancy stems from several factors, such as experimental errors and data collection methods. For instance, the numerical data is derived from the average back surface temperature, while the experimental data is point-measured due to equipment constraints. Nevertheless, both the experimental data and the numerical model indicate that surface temperatures decrease as the time of day progresses.

CONCLUSION

The primary goal of this study was to design a passive cooling system for enhanced photovoltaic efficiency. A monocrystalline PV module was selected and simulated with COMSOL to understand its behavior and to select the optimum cooling system design. A numerical comparison was made between PCM-cooled and the hybrid-cooled systems, from which the hybrid system outperformed the PCM-cooled systems. The hybrid cooled module had a decrease in temperature and a reclaim of the dropped efficiency at the peak temperature during the summer solstice and for the 21st day of each month. Upon comparing the two PV modules. It is recommended when attempting the double layer PCM to check for a wide range of melting temperatures of the available PCM. While this system proved to be numerically effective in Kuwait coordinates, it is recommended to test it at desired locations prior to adopting it.

NOMENCLATURE

q'' = Heat flux
k = Thermal conductivity
h = Heat transfer coefficient
∇T = Temperature gradient
T_p = The panel temperature
T_∞ = Ambient air temperature
T_{sur} = Surroundings temperature
Ts = Surface temperature
ε = Surface emissivity
σ = Stefan Boltzmann constant
η_c = Thermal dependent efficiency
η_{Tref} = The module efficiency at the reference temperature
β_{ref} = The temperature coefficient

REFERENCES

A. AlAjmi, Special Topics in Thermo-Fluid Engineering – ME489. Renewable Energy, Lecture Notes, Kuwait University, 2023.

G. Boyle. Renewable Energy: Power for a Sustainable Future, 2nd ed. Oxford, UK: Oxford University Press, 2004.

Connor, N. (2021, June 29). Glass | Density, Heat Capacity, Thermal Conductivity. Material Properties. Retrieved April 8, 2023, from https://material-properties.org/glass-density-heat-capacity-thermal-conductivity/

Connor, N. (2021, June 30). PET | Density, Strength, Melting Point, Thermal Conductivity. Material Properties. Retrieved April 8, 2023, from https://material-properties.org/pet-density-strength-melting-point-thermal-conductivity.

Comsol 6.0 Documentation. Available: https://doc.comsol.com/6.1/docserver/#!/com.comsol.help.comsol/helpdesk/helpdesk.html. [Accessed 8 March 2023]. Dubey S., Sarvaiya J.N., Seshadri B. Temperature dependent photovoltaic (PV) efficiency and its effect on PV production in the world–a review, Energy Procedia, 33, 2013, pp. 311-321

J. A. Brydson, 1999, Ethylene Vinyl Acetate (EVA): MakeItFrom.com. (2020, May 30). Retrieved April 8, 2023, from https://www.makeitfrom.com/material-properties/Ethylene-Vinyl-Acetate-EVA

Gupta, Arvind. (2014). [Digital Image]. Design And Simulation of Solar Thermal Cooling and Heating System.

Jacobs & Thompson, Foam | EVA | VA35. (2018). In Technical Data Sheet. foamparts.com. Retrieved April 8, 2023, from https://www.foamparts.com/wp-content/uploads/2018/10/va35.pdf

Marko Krstic, Lana Pantic, Stefan Djordjevic, Ivana Radonjic, Veljko Begovic, Branka Radovanovic, Marko Mancic, Passive cooling of photovoltaic panel by aluminum heat sinks and numerical simulation, Ain Shams Engineering, 2023, 2090-4479, https://doi.org/10.1016/j.asej.2023.102330.

M. Chandrasekar, S. Rajkumar, D. Valavan, A review on the thermal regulation techniques for non integrated flat PV modules mounted on building top, Energy and Buildings, 86, 2015, 0378-7788, https://doi.org/10.1016/j.enbuild.2014.10.071.

M. Denchak, *Fossil fuels: The dirty facts, Be a Force for the Future*, nrdc, 2022. [Online]. Available: https://www.nrdc.org/stories/fossil-fuels-dirty-facts#sec-examples. [Accessed 28 April 2023].

Odeh, S., & Behnia, M. (2009). Improving photovoltaic module efficiency using water cooling. Heat Transfer Engineering, 30(6), 499-505.

Perez, J. (2022, November 20). Polycrystalline vs. Monocrystalline Solar Panels: know which is best for your home. Polycrystalline vs. Monocrystalline Solar Panels: know which is best for your home. Retrieved May 2, 2023, from https://www.moserbaersolar.com/blog/polycrystalline-vs-monocrystalline-solar-panels.

S. Chandel and T. Agarwal, Review of cooling techniques using phase change materials for enhancing efficiency of photovoltaic power systems, Renewable and Sustainable Energy Reviews, vol. 73, pp. 1342-1351, 2017.

Tao Ma, Zhenpeng Li, Jiaxin Zhao, Photovoltaic panel integrated with phase change materials (PV-PCM): technology overview and materials selection, Renewable and Sustainable Energy Reviews, 116, 2019, https://doi.org/10.1016/j.rser.2019.109406.

Yun, G.Y., McEvoy, M., Steemers, K., 2007. Design and overall energy performance of a ventilated photovoltaic façade. Solar Energy 81, 383–394. https://doi.org/10.1016/j.solener.2006.06.016.

Zhu, L., Boehm, R.F., Wang, Y., Halford, C., Sun, Y., 2011. Water immersion cooling of PV cells in a high concentration system. Solar Energy Materials and Solar Cells 95, 538–545. https://doi.org/10.1016/j.solmat.2010.08.037.